Large-scale atomistic simulation of quantum effects in $SrTiO_3$ from first principles

Hongyu Wu,[1,2,*] Ri He,[1,*] Yi Lu,[3,4] and Zhicheng Zhong[1,5,†]

[1]*CAS Key Laboratory of Magnetic Materials, Devices and Zhejiang Province Key Laboratory of Magnetic Materials and Application Technology, Ningbo Institute of Materials Technology and Engineering, Chinese Academy of Sciences, Ningbo 315201, China*

[2]*College of Materials Science and Opto-Electronic Technology, University of Chinese Academy of Sciences, Beijing 100049, China*

[3]*Department of Physics, National Laboratory of Solid State Microstructures, Nanjing University, Nanjing 210093, China*

[4]*Collaborative Innovation Center of Advanced Microstructures, Nanjing University, Nanjing 210093, China*

[5]*China Center of Materials Science and Optoelectronics Engineering, University of Chinese Academy of Sciences, Beijing 100049, China*

(Received 23 October 2022; accepted 28 November 2022; published 7 December 2022)

Quantum effects of lattice vibration play a major role in many physical properties of condensed-matter systems, including thermal properties, such as specific heat, structural phase transition, as well as phenomena, such as quantum crystal and quantum paraelectricity that are closely related to zero-point fluctuations. However, realizing atomistic simulations for realistic materials with a fully quantum-mechanical description remains a great challenge. Here, we propose a first-principles strategy for large-scale molecular dynamics simulation, where a high-accuracy force field obtained by deep-potential (DP) is combined with quantum thermal bath (QTB) method to account for quantum effects. We demonstrate the power of this DP+QTB method using the archetypal example $SrTiO_3$, which exhibits several phenomena induced by quantum fluctuations, such as the suppressed structure phase-transition temperature, the quantum paraelectric ground state at low temperatures and the quantum critical behavior $1/T^2$ law of dielectric constant. Our DP+QTB strategy is efficient in simulating large-scale system and is first principles. More importantly, quantum effects of other systems could also be investigated as long as the corresponding DP model is trained. This strategy would greatly enrich our vision and means to study quantum behavior of condensed-matter physics.

DOI: 10.1103/PhysRevB.106.224102

I. INTRODUCTION

Atomic nuclei can be simply treated as classical particles with certain position and velocity, but considering the quantum-mechanical nature of the atomic nuclei, their quantum effects need to be considered in some cases [1]. Based on the hypothesis of energy quantization and Bose-Einstein statistics, collective excitation of atoms can be viewed as the phonon. Based on theory of the phonon, we can calculate thermal conductivity, electrical conductivity, and specific heat of solid. Particularly, at the ground state, the uncertainty principle induces zero-point energy and zero-point fluctuations of atomic position. The zero-point fluctuation is crucial for an accurate description of phenomena, such as quantum crystal, high pressure superconductivity, quantum nature of hydrogen/water, and quantum paraelectricity [2–7]. Although the phonon language has success in describing low temperature, harmonic, and simple systems in q space for many problems that urgently require the atomistic position information in real space and time, such as point effects, dislocations, grain boundary, and the free surface, it is highly desirable to introduce quantum effects in the atomistic simulation of large-scale systems.

The widely accepted method to incorporate quantum mechanics in atomistic simulation is path integral molecular dynamics (PIMD) [8,9]. In PIMD, the nuclei part is mapped to a system composed of several virtual particles connected by a harmonic potential, and its effective Hamiltonian is derived from the Feynman path integral. The PIMD methods have two limitations in practice. The first is the lack of accurate force field. Without an accurate force field, the major part of the calculation is not reliable, and even adding the quantum correction will not give realistic results [10]. Second, extremely expensive calculation costs hinder the practical use of PIMD. PIMD is very time consuming and, consequently, the data applicability(e.g., space scale of the simulation cell, timescale, and time step of simulation) is usually reduced in related work [11]. When it comes to statistics related issues, such as thermodynamic properties, phase diagrams, etc., the results of PIMD are difficult to achieve statistical equilibrium due to scale constraints. Therefore, it is necessary to develop a feasible and *ab initio* numerical scheme to describe the quantum effects in large-scale atomistic simulation.

We propose a deep-potential (DP)+quantum thermal bath (QTB) strategy which can provide quantum correction and yet is capable of large-scale atomistic dynamic simulation with density-functional-theory (DFT) precision. DP is a machine-learning method which can produce accurate force fields of molecular dynamics (MD) by sampling the results of the DFT [12,13]. Some early works in this field have showcased that DP is capable of describing large systems with high

*These authors contributed equally to this work.
†zhong@nimte.ac.cn

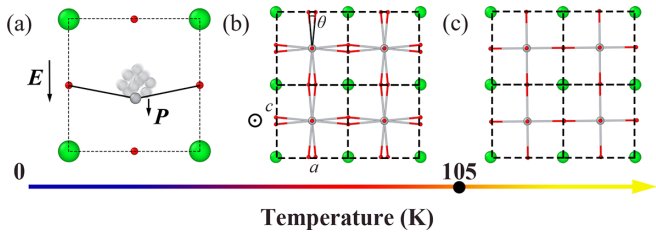

FIG. 1. Schematic of the temperature-dependent structure of $SrTiO_3$ (a) the response of the Ti atom to the electric field at zero temperature, the linear response corresponds to the classical case, and multiple transparent atomic trajectories correspond to the quantum zero-point fluctuation. (b) Tetragonal phase, where a and c are the short and long axes, θ is the rotation angle of the TiO_6 octahedrain each unit cell. (c) Cubic phase where all lattice constants are equal, and θ is zero.

accuracy [14,15]. QTB is a method that preserves the features of quantum statistics in MD [16]. Its core idea is rewriting the fundamental Newtonian equations in MD into Langevin-like equations with colored noise that incorporate quantum statistics. DP+QTB requires a computation cost slightly higher than that of classical MD, so, in principle, can provide results with large space and timescale from which we can obtain sufficient and intuitive physical information.

To demonstrate the power of DP+QTB, we focus on the strontium titanate ($SrTiO_3$). $SrTiO_3$ as a representative ABO_3 perovskite has been reported to exhibit rich physical properties, such as high-mobility electron gas [17], flexoelectricity [18], optically strained metastable ferroelectricity [19], superconducting dome [20], and multiple structural instabilities [21]. What makes it a suitable candidate for testing the DP+QTB method is that its atomic structure has several interesting properties. At low temperatures, the quantum atomic fluctuation stabilizes a paraelectric phase with a high dielectric constant instead of the ferroelectric phase in the classical case [Fig. 1(a)], a phenomenon known as the quantum paraelectricity [6,7,22,23]. With increasing temperatures, $SrTiO_3$ also shows a tetragonal to cubic structural phase transition at about 105 K [Figs. 1(b) and 1(c)].

In this paper, we carried out massive DP+QTB simulations of $SrTiO_3$ up to 135 000 atoms per simulation cell. Compared with classical simulation, DP+QTB shows several qualitative improvements. First, zero-point expansion of the $SrTiO_3$ is observed, which compensates the underestimation of lattice constants in most classical calculations [24]. Second, the tetragonal-to-cubic phase-transition temperature of $SrTiO_3$, which is vastly overestimated in classical simulations, is now much closer to the real transition temperature. Finally, in the quantum critical region at low temperatures, the $1/T^2$ law of the dielectric constant $\varepsilon(T)$ is observed, in agreement with the experimental results and the analytical phenomenological model [6,7].

II. COMPUTATIONAL METHODS

A. Deep potential of $SrTiO_3$

DP is a machine-learning-based method that aims to provide highly applicable and high-accuracy interatomic interaction potentials [12]. The core idea of the DP model is to fit the energy and force of different configurations of certain material through a deep neural network, and its learning samples are a large number of structural configurations (usually these configurations have no more than 50 atoms) and corresponding high-precision DFT reults (energy and force). For a well-trained model, given any corresponding configuration (include those not in the training data and supercells with a large number of atoms), and its total energy, and the force of each atom can be solved with minimal computational cost and at DFT-level accuracy. Thus, the DP model can be applied as a force field in MD simulations.

To obtain the DP model of $SrTiO_3$ we used in this paper, ~2000 candidate configurations which contain information of $SrTiO_3$ were selected for the training dataset. The accuracy of the DP model of $SrTiO_3$ is confirmed in our previous work [15], please refer to the Supplemental Material for the validation of our model (discussion S1 and Tables S1–S3) [25]. The DP predicted energy difference of the tetragonal and cubic phases is 1.008 meV/atom, which is close to the DFT result of ~1.1 meV/atom. Such a subtle variation is crucial for the tetragonal-to-cubic phase transition in $SrTiO_3$. Other properties, such as lattice constant, polarization, elastic constants, and phonon dispersion are tested, and all agree with DFT calculations. For more information about the DP and generation of the dataset, please refer to the Supplemental Material (discussion S1 and Fig. S1) [25].

B. Quantum thermal bath

MD simulations are based on Newtonian mechanics equations and classical statistical theory, therefore, only produce results that conform to classical behavior [26]. QTB is based on the quantum-mechanical fluctuation-dissipation theorem. Instead of treating the atomic nuclei as independent pointlike classical particles, it introduces an associated random force and friction term into the equation, constituting a quantum thermal bath [16]. The equation of motion is modified to the Langevin-like equation,

$$m_i \ddot{r}_{i\alpha} = f_{i\alpha} + R_{i\alpha} - m_i \gamma \dot{r}_{i\alpha}, \tag{1}$$

where m_i is the mass of the ith atom, $r_{i\alpha}$ and $f_{i\alpha}$ are the α (1, 2, or 3) components of the position and the interatomic force exerted by all the other atoms. $R_{i\alpha}$ is the Gaussian random force, and γ is the effective frictional coefficient. The random force spectrum is a colored noise, and its power spectral density $I(\omega)$ is related to γ by the quantum-mechanical fluctuation-dissipation theorem [27],

$$I_{R_{i\alpha}R_{j\beta}}(\omega) = 2m_i\gamma\delta_{ij}\delta_{\alpha\beta}\theta(|\omega|, T), \tag{2}$$

where

$$\theta(\omega, T) = \hbar\omega\left[\frac{1}{2} + \frac{1}{\exp\left(\frac{\hbar\omega}{k_B T}\right) - 1}\right] \tag{3}$$

is the power spectrum of the random force, δ_{ij} and $\delta_{\alpha\beta}$ are the Kronecker symbols, and k_B is the Boltzmann constant. Please refer to the Supplemental Material (discussion S2 and Fig. S2) for details of atomic forces in MD without and with QTB [25]. It is crucial to emphasize that in Eq. (3), the first term $\frac{1}{2}\hbar\omega$, namely, the zero-point energy, has no analog in classical

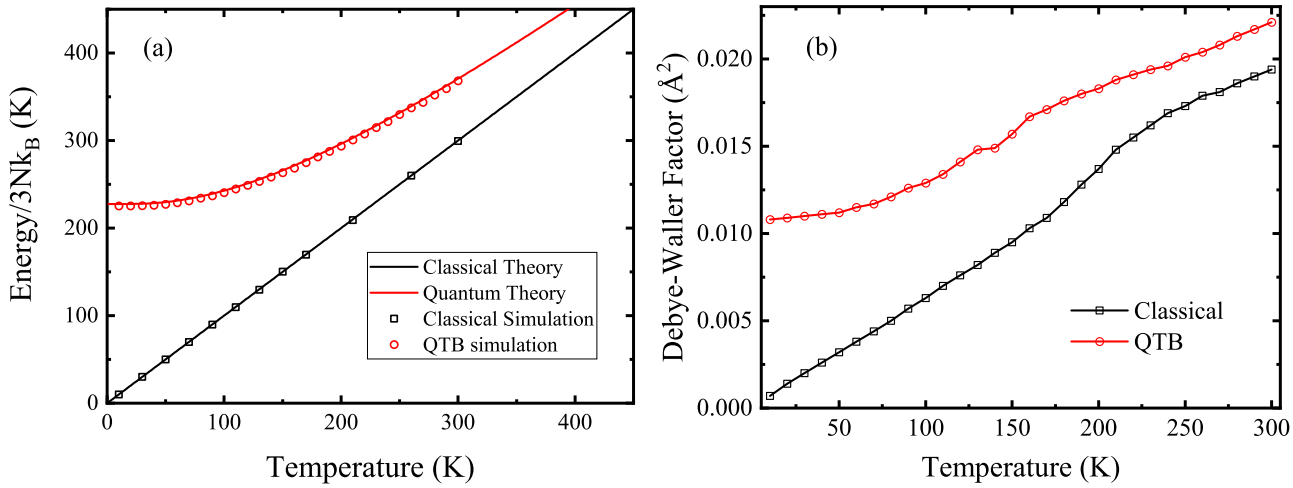

FIG. 2. Comparison of thermodynamic properties between classical and quantum simulations. (a) Average energy per atom in $SrTiO_3$ as a function of temperature. (b) Debye-Waller factor, or average mean-square displacement in $SrTiO_3$ as a function of temperature.

theories. Furthermore, the numerical techniques related to QTB were improved based on simple harmonic oscillators [28], and QTB can be easily manipulated in practice and is independent of the studied system. Previous works have demonstrated that QTB + MD can produce results in good agreement with experiments or PIMD results [16,28,29] with computation complexity comparable to classical MD.

C. Dielectric constant calculation

By adding the effective electric field along the axis of $SrTiO_3$ in MD simulations, we can obtain the dielectric constant via linear-response $\mathbf{P} = \varepsilon\varepsilon_0\mathbf{E}$. The local pseudocubic cell polarization $\mathbf{P}$ can be calculated by atomic displacements with respect to the referenced cubic phase multiplied by the Born effective charges,

$$\mathbf{P} = \sum \mathbf{Z}_i^* \mathbf{u}_i. \tag{4}$$

The components of Born effective charge tensors along the out-of-plane direction were obtained by DFT calculations: $Z^*_{Sr} = 2.54$, $Z^*_{Ti} = 7.12$, $Z^*_{O1} = -5.66$, $Z^*_{O2} = -2.00$, where O1 denotes the oxygen atom in the SrO layer, and O2 denotes the oxygen atom in the TiO_2 layer.

III. RESULTS AND DISCUSSIONS

A. Thermodynamic properties of $SrTiO_3$

The thermodynamic properties are affected by the quantum effects of lattice. By comparing the classical, quantum theoretical, and simulation results, we can, on one hand, test the validity of the DP+QTB method, and, on the other hand, characterize the strength of the quantum effect at any temperature. We first compute the evolution of energy as a function of temperature and show it in the form of $\frac{E}{3Nk_B}$ for a more intuitive display. As shown in Fig. 2(a), the black line and dots represent classical harmonic-oscillator theory and classical MD simulation results, respectively. The energy of $SrTiO_3$ in the classical case are equal to $3Nk_BT$ at any temperature as dictated by the equipartition theorem of classical Boltzmann statistics.

The DP+QTB simulation results are shown by red dots in Fig. 2(a). At 0 K, the energy of system is not 0, which is the zero-point energy. At finite temperature, the increase in energy with the temperature rise in the quantum case is not as high as that in the classical case, which is due to the energy-level gap of quantum excitation, and only part of the phonons contribute to the excitation. At room temperature (300 K), the difference between the classical and the quantum results is still about 70 K in Fig. 2(a), which indicates that even at room temperature, which was previously recognized as a classical scenario, $SrTiO_3$ is still far from the classical limit. The lattice constants and elastic constants of $SrTiO_3$ under classical and quantum conditions to measure the strength of quantum effects as shawn in Table I. Compared to classical MD 0 K or according to the definition of the DP model, it essentially represents the zero-temperature result predicted by DFT, quantum effects are mapped to expansion of lattice constants and reduction of rotation angle θ of TiO_6 octahedrain. As for the elastic constants, quantum effects only slightly affect them.

Based on the theory of the quantum harmonic oscillator, the temperature-dependent energy per atom is given by

$$E(T) = \int_0^\infty g(\omega)\theta(\omega, T)d\omega, \tag{5}$$

TABLE I. Lattice constants and elastic constants of $SrTiO_3$ simluated by classical MD and DP+QTB.

	0 K		300 K	
	Classical	QTB	Classical	QTB
a/Å	3.888	3.904	3.913	3.915
c/Å	3.910	3.914	3.913	3.915
θ/°	5.49	4.75	0	0
C_{11}/GPa	363.18	349.78	340.45	335.45
C_{12}/GPa	106.85	100.33	84.84	80.41
C_{44}/GPa	100.89	101.55	90.34	88.79

TABLE II. T_{zero} of some typical materials (K).

Metal		Covalent		Others	
Al	148.0	B	507.9	Al_2O_3	351.4
Be	346.0	C (diamond)	697.8	LaH_{10}	818.5
Ca	81.6	C (graphene)	666.8	MgO	272.3
Cu	122.4	GaAs	122.6	MoS_2	208.0
Fe	168.2	Si (diamond)	234.6	Na_2SiO_3	288.1
Ta	86.7	SiO_2	398.5	NaCl	102.9
Zr	90.5	$SrTiO_3$	227.5	ZrW_2O_8	270.3

where $g(\omega)$ is the normalized phonon density of states of $SrTiO_3$ as drawn by the red line in Fig. 2(a). The QTB results are able to recover the quantum harmonic approximation and show convergence to the classical limit at high temperatures.

To measure the strength of the quantum effect, we define zero-point temperature $T_{\text{zero}} = \frac{1}{k_B}\int_0^\infty g(\omega)\frac{1}{2}\hbar\omega\, d\omega$, it represents the average energy per atom of zero-point fluctuation in the form of temperature. T_{zero} is about 230 K which is contributed by the zero-point energy of $SrTiO_3$, such a large difference from the classical results suggests that contribution of quantum effects is substantial. We can also determine T_{zero} in other materials to calibrate the strength of quantum effects in the material, T_{zero} of some typical materials are shown in Table II. According to the simple harmonic approximation $\omega = \sqrt{\frac{K}{M}}$, where ω and K are the effective frequency and the spring constant, M is the mass of atom, we can qualitatively analyze T_{zero}. For metals with weak bonding interactions, their effective spring constant K is weaker, and their ω is smaller, so their T_{zero} is generally smaller. On the contrary, in covalent materials, their K is larger, so their T_{zero} is generally larger, which indicates that quantum effects are also strong in these materials. In some special materials, such as LaH_{10} high-pressure hydrogen-rich superconducting material, its effective spring coefficient will be very high because of the special environment under high pressure, and hydrogen is a light element, so the T_{zero} of LaH_{10} is abnormally high. It can be seen from T_{zero} that it is not limited to low temperature and light elements, the quantum effects of many systems are very significant, which also shows the necessity of the quantum effect of MD simulation.

Similar results can also be obtained from the Debye-Waller factor, or the average mean-square displacements of the atom. As shown in Fig. 2(b), the position fluctuations of the atom in the classical case are only contributed by thermal fluctuation, which changes linearly with the temperature and atoms freeze at 0 K. In the quantum case, quantum fluctuation of the atomic position appears at 0 K, suggesting that quantum effects bring about the zero-point motion of 0.0076 $Å^2$, which is contrary to our common sense. The amplitude of the zero-point motion are comparable to thermal fluctuations at about 150 K. And it also returns to the classical limit at high temperatures.

Since the quantum effects have such great influence on the lattice constants and atomic displacement, it naturally affects structural phase transition. $SrTiO_3$ has a structural phase transition from tetragonal to cubic [Figs. 1(b) and 1(c)] when the temperature goes up, both the tetragonal distortion

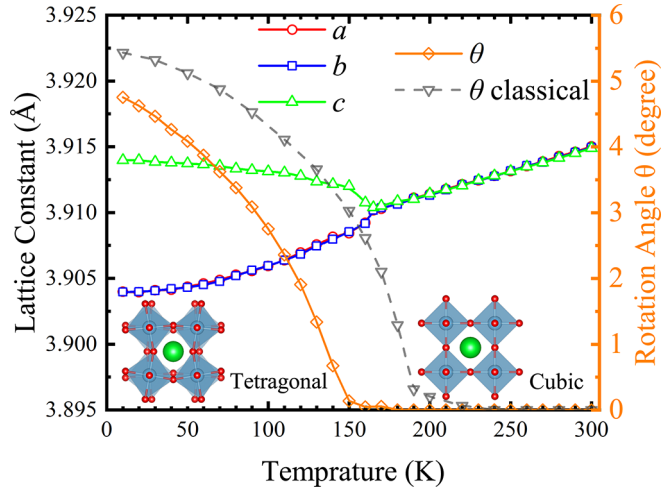

FIG. 3. Average lattice constants and rotation angle of the TiO_6 octahedra around [001] (θ) for $SrTiO_3$ as a function of temperature determined from DP+QTB simulations.

(c/a) and the rotation angle θ of TiO_6 octahedra around [001] decreases with the temperature increase. In our previous work [15], we have already applied the DP model of $SrTiO_3$ and the classical MD to simulate the phase transition of $SrTiO_3$. The classical MD results show that rotation angle θ near 0 K is 5.48° which is larger than experimental result [30]. And the phase-transition temperature is about 200 K, which is also much higher than experimental result 105 K [30]. The temperature-dependent lattice constants and rotation angle simulated by DP+QTB are shown in Fig. 3. θ decreases to 0 at about 160 K, the lattice constants become consistent also around 160 K. It is clear that DP+QTB successfully introduces quantum effects of lattice vibration and, to some extent, more reasonably predicts the phase-transition temperature of $SrTiO_3$.

Although T_{zero} of $SrTiO_3$ is 227.4 K which is higher than transition temperature simulated by classical MD 200 K, results near 0 K ($c/a \neq 1$ and $\theta \neq 0$) indicate that the tetragonal phase is still stable. This means that if the zero-point energy is viewed as the classical temperature, then, it is not simply an increase in temperature, in other words, it is not simply to shift the corresponding temperature. The lattice constants of two short axes (a and b) have a similar behavior to the Debye-Waller factor near 0 K. So the reason for the decrease in the phase-transition temperature compared to classical result is that the quantum fluctuations which exist at finite temperature is remapped, leading to the increase of average displacements and average kinetic energy of atoms, making it easier for atoms to cross the potential barrier to undergo structural transition around 160 K. Although DP+QTB still overestimates the transition temperature compared to the experimental results. This discrepancy might arise the from the accuracy of DFT, the energy difference between two phases is about 1 meV/atom, which varies between different functionals. And since this energy difference is critical to determine the transition temperature, the DP model based on the DFT results will also misestimate the transition temperature.

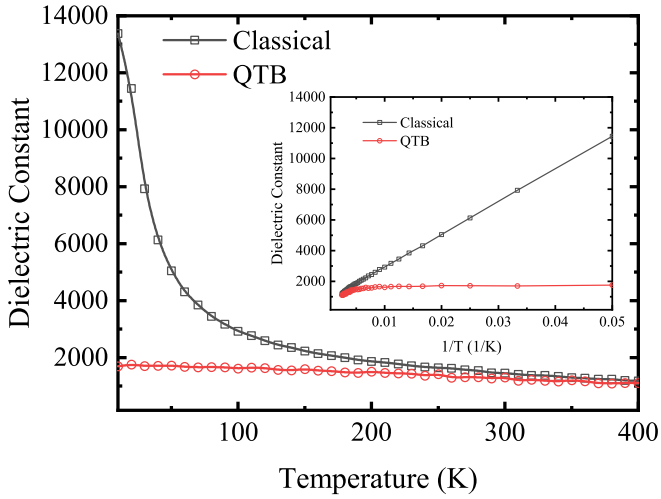

FIG. 4. Dielectric constant simulated by classical and QTB simulations.

B. Dielectric constant of $SrTiO_3$

Another property correlated to quantum effects of lattice vibration in $SrTiO_3$ is the quantum behavior of its dielectric constant at low temperature. According to the phase diagram based on the ϕ^4-quantum field model [schematic phase in Fig. 5(a)] and experimental results [6,7], $SrTiO_3$ exhibits classical behavior at high temperature, the dielectric constant $\varepsilon(T)$ obeys the $\frac{1}{T}$ law. Whereas at finite temperature, the dielectric constant $\varepsilon(T)$ exhibit the nonclassical $\frac{1}{T^2}$ dependence over a wide range of finite temperatures [6,7,31]. In order to fairly show the dielectric constant of $SrTiO_3$ calculated by DP+QTB, we first performed the calculation with classical MD as drawn in black in Fig. 4. Over the entire temperature range, the $\varepsilon(T)$ calculated by classical MD exhibits the $\frac{1}{T}$ law (the inset of Fig. 4), which also means that the dielectric constant at zero temperature will diverge.

As for the $\varepsilon(T)$ simulated by DP+QTB (for more accurate results, the number of atoms in the cell of DP+QTB simulations is 135 000. For a detailed discussion, see Supplemental Material S3 and Fig. S3 [25]) as drawn in red in Fig. 4, it is dramatically different from the classical MD. First, it does not diverge near 0 K but converges to a constant value. Second, its $1/T$ dependence occurs only above 300 K. The possible reason for such a huge difference is that the contribution of thermal fluctuations near 0 K is almost negligible in classical MD, so the highly collective displacement of atoms brought by the electric field is not suppressed, showing extremely strong electrical polarization. And QTB can successfully introduce quantum fluctuations into MD calculations, this fluctuation will be reflected in the position of the atom, so after the time average it can suppress the collective displacement of the atomic affected by the electric field. However, the magnitude of the dielectric constant calculated by QTB in the Fig. 4 is still different from other results [6,7,23,31], and the T^2 law is difficult to characterize. As we mentioned, although $SrTiO_3$ is naturally located near the quantum critical point of the displacive ferroelectrics [P_c in Fig. 5(a)] due to the accuracy of the DFT exchange-correlation function, the lattice constants calculated by DFT are different

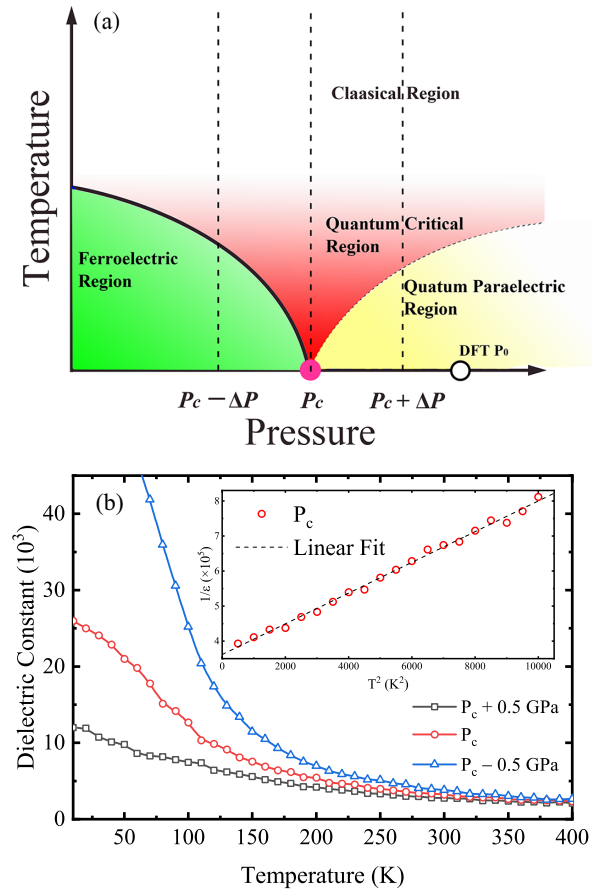

FIG. 5. (a) Schematic phase of displacive ferroelectrics based on ϕ^4-quantum field theory (Ref. [7]). (b) DP+QTB simulations calculated dielectric constant near the quantum critical point of pressure as a function of temperature.

to experimental results, so the DFT simulation result [DFT P_0 in Fig. 5(a)] is far away from quantum critical point P_c. For this problem, we will give a detailed discussion later.

So in order to further explore the dielectric constant of $SrTiO_3$ near the quantum critical point, we apply different sets of hydrostatic pressure in the DP+QTB simulation to make the pressure close to the quantum critical point [P_c is ~ -4.5 GPa]as shown in Fig. 5(b). According to the phase diagram of $SrTiO_3$ [Fig. 5(a)] [7], the applied hydrostatic pressure can be divided into three categories: $P_c - \Delta P$, P_c, and $P_c + \Delta P$. At P_c, as the temperature increases from 0 K, the $SrTiO_3$ undergoes the crossover of two phase regions: the quantum critical region-classical region. $P_c - \Delta P$ and $P_c + \Delta P$ will undergo the ferroelectric region and the quantum paraelectric region first, respectively. When a negative hydrostatic pressure is applied relative to the critical pressure P_c as shown in the inset of Fig. 5(b), $1/\varepsilon(T)$ exhibit the nonclassical $\frac{1}{T^2}$ law over a wide range below 100 K. This again proves that quantum effect of the lattice vibration is not the only matter at 0 K, but also matters in finite temperature, thus, it cannot be overlooked in simulations. Then, we bring out Fig. 6 to illustrate the phase transition at P_c, different types of function fitting are performed for different ranges of data. At a wide range of 0 to 150 K, $\varepsilon(T)$ exhibits the $\frac{1}{T^2}$ law, beyond

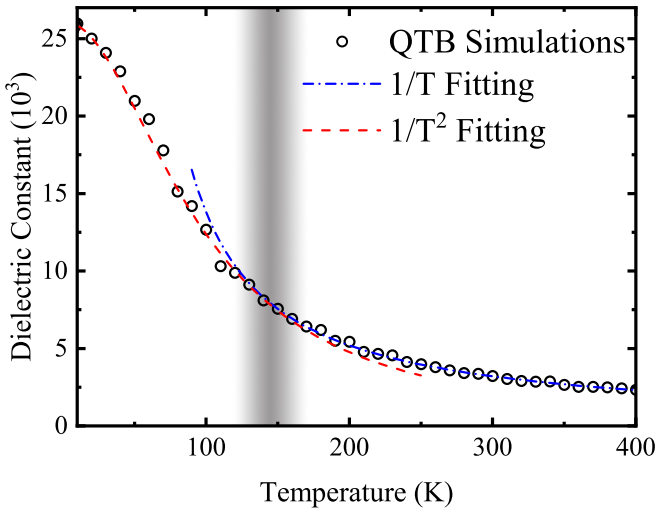

FIG. 6. DP+QTB simulations calculated the dielectric constant at the quantum critical point of pressure as a function of temperature.

150 K $\varepsilon(T)$ returns classical behavior and exhibits the $\frac{1}{T}$ law. It can be concluded that the quantum fluctuations brought by DP+QTB can effectively decay at high temperatures, which indicates that DP+QTB does not bring unphysical results at the classical limit. As for $P_c - \Delta P$, spontaneous ferroelectric polarization occurs at low temperatures, its dielectric constant cannot be represented by the method zone defined in our method. As for $P_c + \Delta P$, a dielectric constant platform occurs at low temperatures. For the above two categories as the temperature increases, the corresponding $\frac{1}{T^2}$ and $\frac{1}{T}$ laws will also appear. At last, we also applied negative pressure to $SrTiO_3$ in classical MD (see the Supplemental Material S4 and Fig. S4 in Ref. [25]), and only the $\frac{1}{T}$ law of the dielectric constant at all temperatures will occur, which shows that classical MD cannot describe the quantum effect.

C. Discussions

Now we discuss the influence of anharmonic effect on our conclusion. Our simulation is carried out by MD simulation at low temperatures and need not involve anharmonic effects. Although the spectral density form of the QTB resembles a simple harmonic approximation [Eq. (3)], it is actually a general result derived from linear-response theory [27]. The results of the QTB using the harmonic potential can strictly conform to the quantum theory of the harmonic oscillator, but this does not mean that the application of the anharmonic potential in the QTB is impossible. The results of the combination of anharmonic potential and QTB are also in good agreement with the theoretically and PIMD results [29], suggesting that the QTB is capable of handling anharmonic effects, so it is expected to describe the situation of high temperatures.

Another question need to be addressed is the discrepancy between rhe DP and the experimental results in the structure phase-transition temperature and DP critical pressure of $SrTiO_3$. First, we have mentioned before that it could originate from the exchange-correlation functionals of DFT. Since the energy difference between the two phases in $SrTiO_3$ is extremely small (∼1 meV), it is extremely difficult for DFT to describe such a subtle energy difference, so there will be a discrepancy in the study of problems related to this energy difference. Second, these widely accepted exchange-correlation functionals, such as the local density approximation, the Perdew-Burke-Ernzerhof (PBE), and PBEsol, they either overestimate or underestimate the experimentally measured lattice constants [32]. Naively, one would expect the ones that predict values closest to the experimental results to be the most accurate functional for the studied material. However, such a point of view should be reexamined as a proper DFT functional intrinsically fails to take into account the zero-point fluctuation, and a "precise" functional should result in a systematic underestimation of lattice constants.

Long-range electrostatic interactions play an important role in studying ferroelectricity, it should be considered in simulation of ferroelectrics in the future. The latest method proves that DP is capable of describing long-range electrostatic interactions [33]. Thus, DP has the potential in simulating other perovskites ferroelectrics.

IV. CONCLUSIONS

We proposed a first-principles method DP+QTB which can deal with large-scale atomistic systems and quantum effects of lattice vibration. DP+QTB is capable of performing efficient large-scale (in both space and time) simulations with DFT accuracy and, thereby, solves an outstanding problem in traditional dynamic simulations, which either adopt a classical description that fully ignores quantum effects, or use methods, such as path-integral molecular dynamics whose application is limited to small systems. DP+QTB can better predict the phase-transition temperature of $SrTiO_3$, and can describe the $\frac{1}{T^2}$ and $\frac{1}{T}$ laws of the $SrTiO_3$ dielectric constant in different temperature ranges where either the quantum or the thermal effects dominate. We define T_{zero} to measure the strength of the quantum effect of the lattice vibration of a material, and we find that the quantum effect of many systems is far from negligible, which suggest that the corresponding research may expand beyond light elements and extremely low temperatures.

ACKNOWLEDGMENTS

H.-Y.W. thanks H.L. for help on Fig. 3 and X.-J.Q. for help on Table II. This work was supported by the National Key R&D Program of China (Grants No. 2021YFA0718900 and No. 2022YFA1403000), the Key Research Program of Frontier Sciences of CAS (Grant No. ZDBS-LY-SLH008), the National Nature Science Foundation of China (Grants No. 11974365 and No. 12204496), the K.C. Wong Education Foundation (Grant No. GJTD-2020-11), and the Science Center of the National Science Foundation of China (Grant No. 52088101). Y.L. acknowledges support from the National Natural Science Foundation of China under Grant No. 12274207 and the Ministry of Science and Technology of China under Grant No. 2022YFA1403000.

[1] C. Kittel, P. McEuen, and P. McEuen, *Introduction to Solid State Physics* (Wiley, New York, 1996), Vol. 8.

[2] C. Cazorla and J. Boronat, Rev. Mod. Phys. **89**, 035003 (2017).

[3] I. Errea, F. Belli, L. Monacelli, A. Sanna, T. Koretsune, T. Tadano, R. Bianco, M. Calandra, R. Arita, F. Mauri *et al.*, Nature (London) **578**, 66 (2020).

[4] J. A. Morrone and R. Car, Phys. Rev. Lett. **101**, 017801 (2008).

[5] X.-Z. Li, B. Walker, and A. Michaelides, Proc. Natl. Acad. Sci. USA **108**, 6369 (2011).

[6] K. A. Müller and H. Burkard, Phys. Rev. B **19**, 3593 (1979).

[7] S. Rowley, L. Spalek, R. Smith, M. Dean, M. Itoh, J. Scott, G. Lonzarich, and S. Saxena, Nat. Phys. **10**, 367 (2014).

[8] D. Marx and M. Parrinello, Z. Phys. B: Condens. Matter **95**, 143 (1994).

[9] D. Marx and M. Parrinello, J. Chem. Phys. **104**, 4077 (1996).

[10] W. H. Miller, Proc. Natl. Acad. Sci. USA **102**, 6660 (2005).

[11] D. M. Ceperley, Rev. Mod. Phys. **67**, 279 (1995).

[12] L. Zhang, J. Han, H. Wang, R. Car, and W. E., Phys. Rev. Lett. **120**, 143001 (2018).

[13] L. Zhang, J. Han, H. Wang, W. A. Saidi, R. Car, and W. E., End-to-end symmetry preserving inter-atomic potential energy model for finite and extended systems, in *Proceedings of the 32nd International Conference on Neural Information Processing Systems*, NIPS'18 (Curran Associates, Red Hook, NY, 2018), pp. 4441–4451.

[14] L. Zhang, H. Wang, R. Car, and W. E., Phys. Rev. Lett. **126**, 236001 (2021).

[15] R. He, H. Wu, L. Zhang, X. Wang, F. Fu, S. Liu, and Z. Zhong, Phys. Rev. B **105**, 064104 (2022).

[16] H. Dammak, Y. Chalopin, M. Laroche, M. Hayoun, and J.-J. Greffet, Phys. Rev. Lett. **103**, 190601 (2009).

[17] A. Ohtomo and H. Y. Hwang, Nature (London) **427**, 423 (2004).

[18] P. Zubko, G. Catalan, A. Buckley, P. R. L. Welche, and J. F. Scott, Phys. Rev. Lett. **99**, 167601 (2007).

[19] T. F. Nova, A. S. Disa, M. Fechner, and A. Cavalleri, Science **364**, 1075 (2019).

[20] J. M. Edge, Y. Kedem, U. Aschauer, N. A. Spaldin, and A. V. Balatsky, Phys. Rev. Lett. **115**, 247002 (2015).

[21] W. Zhong and D. Vanderbilt, Phys. Rev. Lett. **74**, 2587 (1995).

[22] P. Chandra, G. G. Lonzarich, S. Rowley, and J. Scott, Rep. Prog. Phys. **80**, 112502 (2017).

[23] D. Shin, S. Latini, C. Schäfer, S. A. Sato, U. De Giovannini, H. Hübener, and A. Rubio, Phys. Rev. B **104**, L060103 (2021).

[24] R. B. Wexler, Y. Qi, and A. M. Rappe, Phys. Rev. B **100**, 174109 (2019).

[25] Sea Supplemental Material at http://link.aps.org/supplemental/10.1103/PhysRevB.106.224102 for discussions s1–s5, Figs. s1– s5, Tables s1– s5, and Refs. [34,35].

[26] S. Plimpton, J. Comput. Phys. **117**, 1 (1995).

[27] H. B. Callen and T. A. Welton, Phys. Rev. **83**, 34 (1951).

[28] J.-L. Barrat and D. Rodney, J. Stat. Phys. **144**, 679 (2011).

[29] H. Dammak, M. Hayoun, Y. Chalopin, and J.-J. Greffet, Phys. Rev. Lett. **107**, 198902 (2011).

[30] K. A. Müller and W. Berlinger, Phys. Rev. Lett. **26**, 13 (1971).

[31] M. J. Coak, C. R. Haines, C. Liu, S. E. Rowley, G. G. Lonzarich, and S. S. Saxena, Proc. Natl. Acad. Sci. USA **117**, 12707 (2020).

[32] P. Haas, F. Tran, and P. Blaha, Phys. Rev. B **79**, 085104 (2009).

[33] L. Zhang, H. Wang, M. C. Muniz, A. Z. Panagiotopoulos, R. Car, and W. E., J. Chem. Phys. **156**, 124107 (2022).

[34] Y. Zhang, H. Wang, W. Chen, J. Zeng, L. Zhang, H. Wang, and W. E., Comput. Phys. Commun. **253**, 107206 (2020).

[35] J. P. Perdew, K. Burke, and M. Ernzerhof, Phys. Rev. Lett. **78**, 1396(E) (1997).